Planta (2013) 238:283–291
DOI 10.1007/s00425-013-1888-y

ORIGINAL ARTICLE

The vacuolar channel VvALMT9 mediates malate and tartrate accumulation in berries of *Vitis vinifera*

Alexis De Angeli · Ulrike Baetz · Rita Francisco · Jingbo Zhang · Maria Manuela Chaves · Ana Regalado

Received: 22 January 2013 / Accepted: 21 April 2013 / Published online: 5 May 2013

Abstract *Vitis vinifera* L. represents an economically important fruit species. Grape and wine flavour is made from a complex set of compounds. The acidity of berries is a major parameter in determining grape berry quality for wine making and fruit consumption. Despite the importance of malic and tartaric acid (TA) storage and transport for grape berry acidity, no vacuolar transporter for malate or tartrate has been identified so far. Some members of the aluminium-activated malate transporter (ALMT) anion channel family from *Arabidopsis thaliana* have been shown to be involved in mediating malate fluxes across the tonoplast. Therefore, we hypothesised that a homologue of these channels could have a similar role in *V. vinifera* grape berries. We identified homologues of the Arabidopsis vacuolar anion channel AtALMT9 through a TBLASTX search on the *V. vinifera* genome database. We cloned the closest homologue of AtALMT9 from grape berry cDNA and designated it VvALMT9. The expression profile revealed that VvALMT9 is constitutively expressed in berry mesocarp tissue and that its transcription level increases during fruit maturation. Moreover, we found that VvALMT9 is targeted to the vacuolar membrane. Using patch-clamp analysis, we could show that, besides malate, VvALMT9 mediates tartrate currents which are higher than in its Arabidopsis homologue. In summary, in the present study we provide evidence that VvALMT9 is a vacuolar malate channel expressed in grape berries. Interestingly, in *V. vinifera*, a tartrate-producing plant, the permeability of the channel is apparently adjusted to TA.

Keywords Anion transport · Grape berry ripening · Ion channel · Malic acid · Tartaric acid · Vacuole

Abbreviations

ALMT	Aluminium-activated malate transporter
MA	Malic acid
TA	Tartaric acid
SUC	Succinic acid
AA	L-Ascorbic acid
PEPC	Phosphoenolpyruvate carboxylase
MDH	Malate dehydrogenase
ME	Malic enzyme
AttDT	*Arabidopsis thaliana* tonoplast dicarboxylate transporter
DAF	Days after flowering

Introduction

Grape berries (*Vitis vinifera* L.) exhibit a double-sigmoid growth pattern that results from two successive periods of vacuolar swelling during which the nature of accumulated solutes changes significantly (Coombe 1992). During the first period, called green or herbaceous stage, berries accumulate mainly organic acids in the vacuole [predominantly malic acid (MA) and tartaric acid (TA)] and have a constant vacuolar pH of 2.5 (Terrier et al. 2001). At the onset of ripening (*véraison*), berries often become coloured

A. De Angeli and U. Baetz contributed equally to the work.

A. De Angeli (✉) · U. Baetz · R. Francisco · J. Zhang
Institute of Plant Biology, University of Zurich, Zollikerstr. 107, 8008 Zurich, Switzerland
e-mail: alexis.deangeli@botinst.uzh.ch; deangeli.alexis@gmail.com

R. Francisco · M. M. Chaves · A. Regalado
Instituto de Tecnologia Química e Biológica, Universidade Nova de Lisboa, Av. da República, 2780-157 Oeiras, Portugal

and start to accumulate sugars. At maturity, the concentrations of glucose and fructose may be higher than 1 M (Coombe 1976; Terrier et al. 2001). In parallel, their organic acid content decreases, whereby the vacuolar pH increases to about 3.5 (Terrier et al. 2001). Tartaric and malic acid generally account for 69–92 % of all organic acids in grape berries, and both of them reach maximal concentrations at the end of the green stage (Conde et al. 2007). However during ripening, the content of MA in berries continuously decreases, while that of TA remains constant. The acidity of berries is a major parameter determining their quality. The overall consumer appreciation is more related to the titratable acidity/sugar content than to the soluble sugars alone. Besides flavour and colour, the pH of grapes at harvest is a critical parameter for vinification. Wine pH depends on three major factors: the total amount of acids, the ratio of MA to TA and the concentration of potassium (Conde et al. 2007).

Despite their similar chemical nature, MA and TA synthesis follow different pathways. The biosynthesis of TA starts with L-ascorbic acid (AA) and is still not fully understood (Saito and Kasai 1969). The accumulation of TA resulting in high levels in mature berries suggests a strongly active metabolic pathway that may compete for AA with redox-associated functions more commonly linked to in vivo AA pools (Melino et al. 2009). In contrast, the precursor of MA is sucrose which is translocated from the leaves to the green berries. The main enzymes involved in malate synthesis (phosphoenolpyruvate carboxylase, PEPC and malate dehydrogenase, MDH) have been identified and shown to be active in grape berries (Taureilles-Saurel et al. 1995a, b; Fernie and Martinoia 2009; Sweetman et al. 2009). Instead, the decrease in acid content during grape berry ripening has been mainly associated with mitochondrial malate oxidation, most likely by malic enzyme (ME) (Kanellis and Roubelakis-Angelakis 1993).

Tonoplast transporters of MA and dicarboxylic acids have long been sought given the imperative vacuolar storage of these compounds. Emmerlich et al. (2003) identified the *Arabidopsis thaliana* tonoplast dicarboxylate transporter (*At*tDT) in mesophyll cells at the molecular level. Subsequently, members of the aluminium-activated malate transporter (ALMT) gene family (*A. thaliana* ALMT9 and 6) were identified to encode vacuolar malate channels in mesophyll and guard cells (Kovermann et al. 2007; Meyer et al. 2011).

The amount of MA and TA has a fundamental impact on grape berry quality for the wine-making industry (Conde et al. 2007). Despite the importance of MA and TA transport processes in grape berries, no vacuolar transporter for malate has been identified in *V. vinifera* until now and to the best of our knowledge no tartrate transporter/channel has been reported in plants. Therefore, in the present work we tried to fill this lack of information aiming at identifying a malate/tartrate transporter in *V. vinifera*. We hypothesised that an *At*ALMT9 homologue could code for a vacuolar malate/tartrate channel in grape berries. Here, we describe the cloning and characterisation of a grape berry ALMT (*V. vinifera* ALMT). We identify VvALMT9 and show that it is able to mediate malate and tartrate accumulation in the vacuole of grape berries.

Materials and methods

Plant material

Berry samples (*V. vinifera* cv. Aragonez) were collected from an experimental plot at the commercial vineyard Monte dos Seis Reis (South of Portugal, Estremoz, Portugal). Berries were collected during the summer season of 2007 in pre-*véraison* (49DAF), *véraison* (68DAF), maturation (81 DAF) and full maturation stage (97 DAF). Collected berries were immediately frozen in liquid nitrogen and stored at −80 °C before usage.

Molecular cloning of VvALMT9

Total RNA was extracted from mature mesocarp (pulp) tissues using the method of Reid et al. (2006). Mesocarp tissue was ground in liquid nitrogen to a fine powder and immediately added to pre-warmed RNA extraction buffer. RNA was purified using the RNeasy kit (Qiagen) in the presence of DNaseI according to manufacturer's instructions (RNase-Free DNase Set; Qiagen). Full-length cDNAs were synthesised using RT included in the LongRange 2Step RT-PCR kit (Qiagen) according to the manufacturer's instructions. VvALMT9 full-length cDNA was amplified using the high fidelity DNA polymerase Phusion™ (Finnzymes). The resulting PCR product was cloned into pDONR™ 221 as entry vector and pH7FWG2™ as destination vector (Gateway® Technology, Invitrogen).

Phylogenetic analysis

The *V.vinifera* genome (http://www.cns.fr/spip/Vitis-vinifera-e.html), phytozome (http://www.phytozome.net) and the National Center for Biotechnology Information (NCBI; http://www.ncbi.nlm.nih.gov/) databases were screened using *At*ALMT9 (At3g18440) as query to find homologous grapevine sequences. Multiple sequence alignments were performed with the ClustalW algorithm (http://align.genome.jp/) using default parameters (Thompson et al. 1994). The phylogenetic analysis was performed with the phylogeny software (http://www.phylogeny.fr).

Overexpression of VvALMT9-GFP and AtALMT9-GFP in *Nicotiana benthamiana*

For transient overexpression (Kovermann et al. 2007) of VvALMT9-GFP and AtALMT9-GFP, the cDNA was cloned into pH7FWG2™ or the pART27 vector, respectively. The *Agrobacterium*-mediated infiltration of *N. benthamiana* leaves was performed as described with slight modifications (Holsters et al. 1980). After *Agrobacterium*-mediated infiltration, tobacco plants were grown in the greenhouse (16 h light/8 h dark, 25 °C). 2–3 days after the *Agrobacterium*-mediated infiltration, the transformed leaves were used to extract protoplasts and vacuoles for confocal microscopy and patch-clamp experiments. *N. benthamiana* seeds were derived from own stocks.

Intracellular localisation of VvALMT9-GFP

Protoplasts and vacuoles of *N. benthamiana* leaves overexpressing VvALMT9-GFP were isolated as described for patch-clamp experiments. Microscopy was conducted using a Leica DMIRE2 (http://www.leica-microsystems.com) laser scanning microscope. The microscope was equipped with a 63× glycerol objective. For image acquisition, the appropriate Leica confocal software was used. GFP fluorescence was imaged at an excitation wavelength of 488 nm, and the emission signal was detected between 500 and 530 nm.

Gene expression of VvALMTs

Total RNA was extracted from 150 mg grape berry pulp (mesocarp) using the RNeasy Plant Mini Kit (Qiagen) following the manufacturer's instructions. An on-column DNase I digestion step was included. Total RNA (1 µg) was reverse transcribed using M-MLV reverse transcriptase (Promega) and oligo (dT) priming. Transcript levels were determined by quantitative real-time PCR using the 7500 Fast Real-Time PCR System (Applied Biosystems) with the 7500 Software version 2.0.4. Reactions were performed in a final volume of 20 µL with 5 µL cDNA (diluted 1:10), 0.25 µM gene-specific primers and 10 µL SYBR Green PCR Master Mix (Applied Biosystems). Reaction conditions for the thermal cycling were as follows: after enzyme activation at 95 °C for 10 min, amplification was carried out in a two-step PCR procedure with 40 cycles of 15 s at 95 °C for denaturation and 1 min at 60 °C for annealing/extension. All reactions were performed in technical triplicates of three biological replicates. Gene primer sequences used in the qRT-PCR analyses were as follows: VvALMT5 forward 5′-GAGTGCCAGCTCCTTGTCTT-3′, VvALMT5 reverse 5′-TTTTGGAGCTGGAAGGTCCG-3′; VvALMT6 forward 5′-GAAACAATCCCCTTGGCCCT-3‘, VvALMT6 reverse 5′-ACATTTTGGAGCCTGGCAAC-3‘; VvALMT9 forward 5′-TGAATTTGTTGCGAGGCTTCA-3′, VvALMT9 reverse 5′-CACCTGCGCAATCTTGTTCC-3′; VvALMT13 forward 5′-CCTTGCCACCTTCACTTCCT-3′, VvALMT13 reverse 5′-CACTGCAAGCTGGTCAACTG-3′. Dissociation curves were analysed to verify the specificity of each amplification reaction; the dissociation curve was obtained by heating the amplicon from 60 to 95 °C. Transcript levels were calculated using the standard curve method and normalised against the VvActin gene (GU585869) as described by (Pfaffl 2001).

Protoplast preparation and patch-clamp recordings on isolated vacuoles

Tobacco leaves were gently scratched on the abaxial side and floated in the enzymatic solution for 30–45 min at 30 °C. The enzyme solution contained 0.3 % (w/v) cellulase R-10, 0.03 % (w/v) pectolyase Y-23, 1 mM $CaCl_2$, 500 mM sorbitol and 10 mM Mes, pH 5.3. Protoplasts were washed twice and resuspended in solution without enzymes. Vacuoles were isolated by calcium and osmotic shock. Membrane currents were recorded using the patch-clamp technique as described elsewhere (Meyer et al. 2011). Briefly, currents were recorded with an EPC10 patch-clamp amplifier (HEKA electronics) using the Patchmaster software (HEKA Electronics, Lambrecht/Pfalz, Germany). Data were analysed with the FitMaster software (HEKA electronics). Following the formation of giga seals between the patch pipette and the vacuolar membrane, the excised vacuole-side-out patches were obtained after having established the whole-vacuole configuration by pulling the pipette away from the vacuole. Pipette solutions contained 112 mM MA, 5 mM HCl and 3 mM $MgCl_2$ adjusted to pH 6.0 with 100 mM 1,3-bis[tris(hydroxymethyl)methylamino]propane (BTP). The standard bath solution contained 100 mM MA, 160 mM BTP, 3 mM $MgCl_2$ and 0.1 mM $CaCl_2$, pH 7.5. For selectivity studies, MA in the standard bath solution was replaced by equimolar amounts of TA. The osmotic pressure of all solutions was 550 mOsm adjusted with D-sorbitol. Ionic solutions bathing the vacuole were exchanged by a gravity-driven perfusion system coupled to a peristaltic pump. Current–voltage characteristics were either obtained by subtracting the current at $t = 0$ from the quasi-stationary currents (averaging the last 50 ms of the current trace) elicited by main pulses; or from the value of the tail currents (at $t = 0$) fitted by a monoexponential function. Error bars represent standard error throughout the article.

Results

Cloning VvALMT9, a homologue of the Arabidopsis vacuolar channel AtALMT9 from *Vitis vinifera*

Since two members of the ALMT family from *A. thaliana* (AtALMT9 and 6; Kovermann et al. 2007; Meyer et al. 2011) have been demonstrated to mediate malate fluxes across the tonoplast, we hypothesised that ALMTs could have a similar role in *V. vinifera* berries. To identify a homologue of the Arabidopsis vacuolar anion channel AtALMT9 (At3g18440; Kovermann et al. 2007), we performed a TBLASTX search on the genome database of *V. vinifera* (http://www.phytozome.net) using the cDNA of this channel as a query. The search identified five sequences displaying a significant similarity to *AtALMT9* (e value $\leq 10^{-30}$). We found that the genomic sequence GSVIVG01008270001 exhibited the highest degree of similarity (e value $= 10^{-161}$). We cloned the grape berry cDNA of the closest homologue of *AtALMT9* from mRNA extracted from the mesocarp of grape berries and designated it *VvALMT9* (Fig. 1). The alignment of the cloned cDNA sequence with the Vitis genome revealed that the *VvALMT9* gene consisted of six exons coding for a protein of 588 amino acids. VvALMT9 displays a high degree of identity with AtALMT9 (64 %). To further analyse the ALMT family in *V. vinifera* we performed additionally a BLAST search on the Vitis proteome (http://www.phytozome.net) using the AtALMT9 amino acid sequence. A dendrogram based on the amino acid similarity indicates that the 13 members of the ALMT family in *V. vinifera* are grouped in three clades as in Arabidopsis (Fig. 1). Notably, even if the total number of ALMTs is similar in Arabidopsis (14 members) and Vitis (13 members), the number of members per clade is different between the two species. Clade I, to which AtALMT1 (Hoekenga et al. 2006) belongs, contains in *V. vinifera* eight members, while it includes five members in *A. thaliana*. Clade II is represented in *V. vinifera* by four members. In contrast, in *A. thaliana* clade II contains five members including AtALMT9 and 6 (Kovermann et al. 2007; Meyer et al. 2011). Interestingly, clade III incorporates only one member in *V. vinifera*, whereas in Arabidopsis there are four members, amongst them AtALMT12 (Meyer et al. 2010).

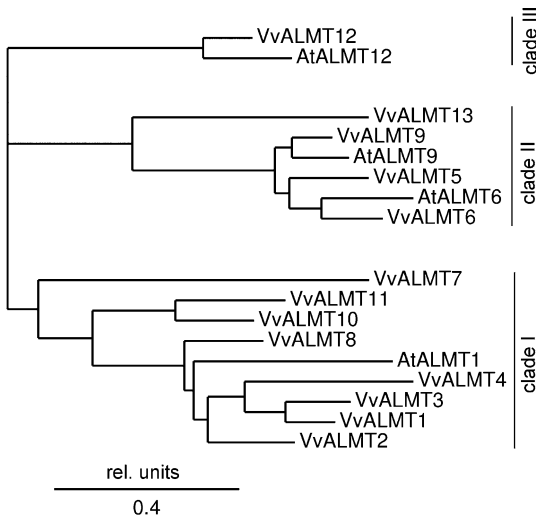

Fig. 1 Dendrogram of the ALMT protein family in *V. vinifera*. Based on multiple amino acid sequence alignments using ClustalW (Thompson et al. 1994) the 13 members of the VvALMT protein family were classified into three main clades as in *A. thaliana*. Clade I members: VvALMT1, VvALMT2, VvALMT3, VvALMT4, VvALMT7, VvALMT8, VvALMT10 and VvALMT11 (GSVIVT01036162001, GSVIVT01037570001, GSVIVT01037569001, GSVIVT01036157001, GSVIVT01011122001, GSVIVT01011148001, GSVIVT01019627001, GSVIVT01027186001). Clade II members: VvALMT5, VvALMT6, VvALMT9 and VvALMT13 (GSVIVT01011922001, GSVIVT01011922001b, GSVIVT01008270001, GSVIVT01019447001). Clade III: VvALMT12 (GSVIVT01013184001). The ALMTs from *A. thaliana* that have been already characterised are inserted in the dendrogram. Branch lengths are given in relative units illustrating the level of occurred evolutionary change

VvALMT9 expression levels increase during grape berry development

To elucidate whether the members of VvALMT clade II including VvALMT9 could feature physiological relevance during fruit development and maturation, we conducted expression profile analysis using quantitative real-time PCR. On that purpose, grape berry mesocarp tissue was used to extract RNA at different developmental stages of the fruit. Despite not detecting significant expression levels for VvALMT6 and marginal transcription of VvALMT13 in this tissue, the other clade members VvALMT9 and VvALMT5 were substantially transcribed in berries at all examined stages (Fig. 2). In the green phase (49 days after flowering, DAF) and at the onset of ripening (68 DAF) transcript levels of VvALMT9 were lower relative to the fully developed fruit. After induction of the ripening process (81 and 97 DAF), expression levels rose approximately four times. VvALMT13 showed generally a less pronounced expression magnitude than VvALMT9, but a similar tendency of transcriptional up-regulation during fruit development. In contrast, VvALMT5 was constantly highly expressed throughout maturation, therefore representing the prevalent member of clade II VvALMTs in grape berries. Thus, with the expression profile we demonstrate that VvALMTs are constitutively transcribed in grape mesocarp tissue. Further, VvALMT9 transcript levels experience a marked increase throughout the ripening process. Altogether, these results suggest that clade II VvALMTs might be involved in grape berry maturation.

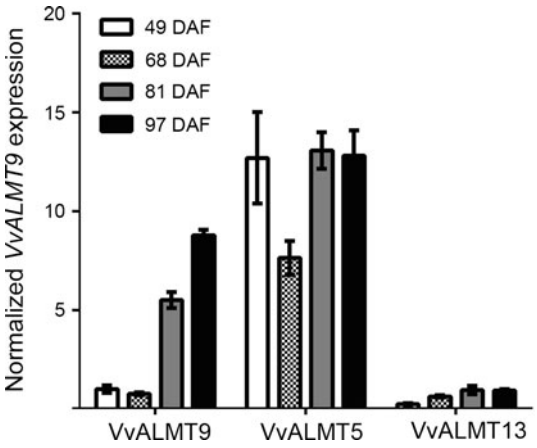

Fig. 2 Quantitative real-time PCR expression profile of VvALMTs in grape berry mesocarp. Displayed are expression profiles of VvALMT9, VvALMT5 and VvALMT13 in mesocarp tissue during fruit development and ripening (49–97 days after flowering, DAF). VvActin (GU585869) served as a reference gene. Relative expression levels of VvALMTs were normalised to VvALMT9 at 49 DAF. Results represent the mean ± standard deviation (SD) of three biological replicates

VvALMT9 is localised in the tonoplast

To investigate the subcellular localisation of VvALMT9, we generated a construct encoding the VvALMT9 protein with a C-terminal GFP fusion in pH7FWG2 (Gateway® Technology, Invitrogen). Subsequently, we transiently expressed VvALMT9 in *N. benthamiana* leaves by agro-infiltration (Holsters et al. 1980). Confocal laser scanning microscopy analysis of vacuoles extracted from lysed protoplasts of transiently transformed tobacco leaves allowed localising VvALMT9-GFP in the tonoplast (Fig. 3a). These data indicate that VvALMT9 is targeted to the vacuolar membrane as its counterpart in Arabidopsis.

VvALMT9 is an ionic channel mediating malate currents

The localisation of VvALMT9 in the tonoplast allowed using the patch-clamp technique to characterise the properties of the putative ion channel. Electrophysiological experiments were conducted on vacuoles obtained from *N. benthamiana* protoplasts transiently transformed with the VvALMT9-GFP construct. Vacuoles expressing VvALMT9-GFP were selected by their fluorescence signal under the microscope and chosen for patch-clamp experiments in excised cytosolic-side-out configuration (i.e. with the cytosolic side of the membrane exposed to the bath solution). As a first step we compared the currents that could be measured in vacuoles from excised patches from non-transformed and transformed cells (Fig. 3b). We found that in symmetric malate concentrations (100 mM $malate^{2-}_{cyt}$ and 100 mM $malate^{2-}_{vac}$), patches from

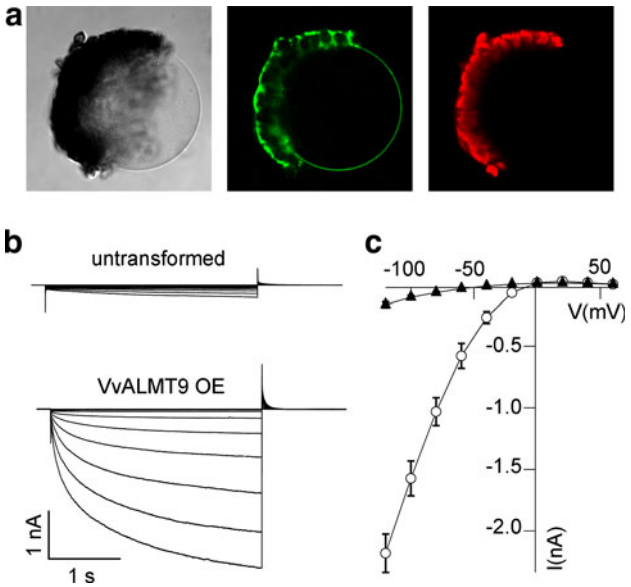

Fig. 3 Intracellular localisation and anion conductivity of VvALMT9-GFP. **a** Transmission, GFP fluorescence and chlorophyll autofluorescence images showing the tonoplastic localisation of VvALMT9-GFP in an isolated vacuole after lysis of *N. benthamiana* protoplasts which transiently overexpressed VvALMT9-GFP. **b** Representative malate current recordings of non-transformed and VvALMT9-GFP overexpressing vacuoles obtained from patches in excised cytosolic-side-out configuration. Currents were elicited with 3 s voltage pulses ranging from +60 to −120 mV in −20 mV steps followed by a 1.5 s tail pulse at +60 mV. The holding potential was +60 mV. **c** Mean current–voltage relationships of vacuolar patches of non-transformed (*filled triangles*; $n = 4$) and VvALMT9-GFP over-expressing (*open circles*; $n = 7$) protoplasts in symmetrical malate conditions $\left(100\,\text{mM}\ malate^{2-}_{cyt}/100\,\text{mM}\ malate^{2-}_{vac}\right)$. *Error bars* represent ±SE

fluorescent vacuoles displayed a voltage-dependent inward current with a time of half activation of $t_{1/2} = 290 \pm 20$ ms reminiscent of the currents observed in AtALMT9 and AtALMT6 overexpressing vacuoles (Kovermann et al. 2007; Meyer et al. 2011). In patches of transformed vacuoles, we measured current amplitudes of -1.6 ± 0.2 nA, while in patches from non-transformed vacuoles the detected amplitudes were -0.10 ± 0.01 nA at −100 mV (Fig. 3c). The ten times higher currents found in patches from transiently transformed vacuoles indicate that VvALMT9 is able to mediate ionic currents across the tonoplast. To verify whether the currents observed in VvALMT9 transformed vacuoles are mediated by malate, we switched the cytosolic side solution from 100 mM $malate^{2-}_{cyt}$ to 10 mM $malate^{2-}_{cyt}$ and followed the reversal potential and the change in current amplitude (Fig. 4). During the exchange of the cytosolic side solution, the currents mediated by VvALMT9 decreased from -1.6 ± 0.2 nA in 100 mM $malate^{2-}_{cyt}$ to -0.19 ± 0.09 nA in 10 mM $malate^{2-}_{cyt}$ at −100 mV (Fig. 4b). In 100 mM $malate^{2-}_{cyt}$ and

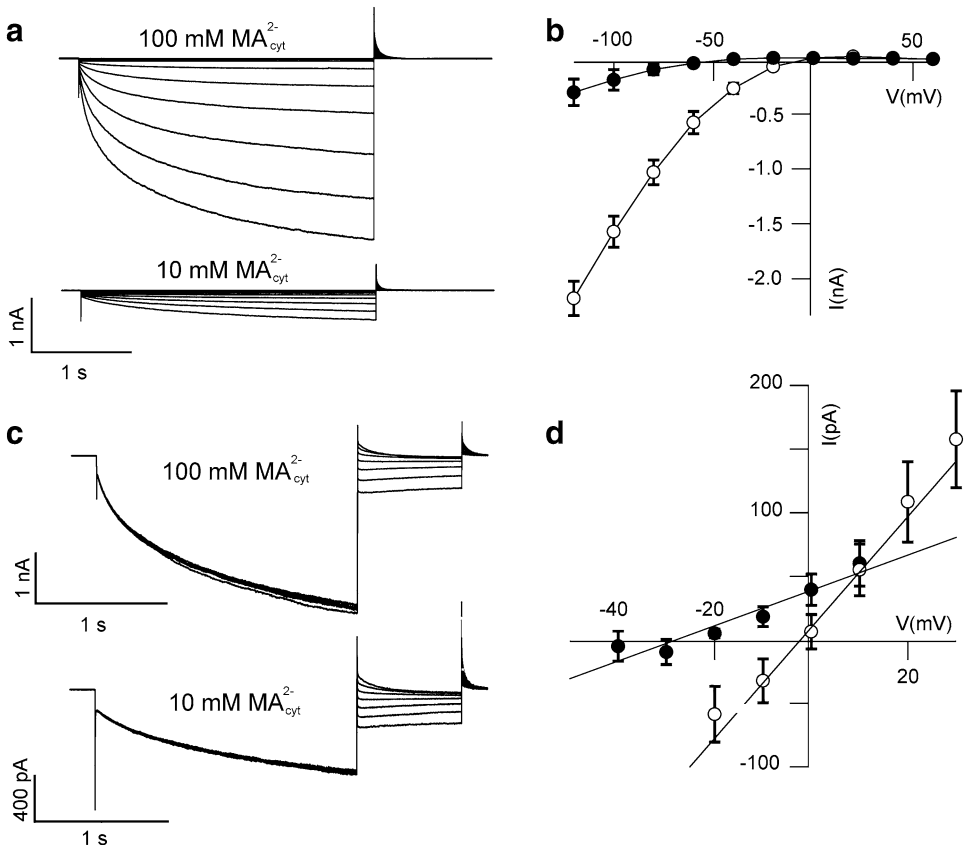

Fig. 4 Analysis of malate inward fluxes across the tonoplast mediated by VvALMT9. **a** Representative current traces measured in excised cytosolic-side-out patches of VvALMT9-overexpressing vacuoles in the presence of 100 mM cytosolic malate and after the exchange to a 10 mM cytosolic malate solution at different applied membrane potentials. Currents were elicited with 3 s voltage pulses ranging from +60 to −120 mV in −20 mV steps followed by a 1.5 s tail pulse at +60 mV. The holding potential was +60 mV. **b** I–V curves comparing the voltage-dependent inward current of VvALMT9 between 100 mM (*open circles*; $n = 7$) and 10 mM (*filled circles*; $n = 7$) cytosolic malate concentrations. **c** Current traces representing the tail current of patches in 100 and 10 mM malate at the cytosolic side. Currents were elicited by an activating pre-pulse at −100 mV (2 s), followed by a series of test pulses ranging from +30 to −20 mV (100 mM MA^{2-}_{cyt}) and +10 to −40 mV (10 mM MA^{2-}_{cyt}) in −10 mV steps (1 s). The holding potential was at +60 mV. **d** Corresponding reversal potentials obtained from a linear fit of the mean current–voltage relations of instantaneous tail currents from patches of vacuoles overexpressing VvALMT9 in 100 mM (*open circles*; $n = 4$) and 10 mM malate (*filled circles*; $n = 4$) in the cytosolic bath solution. The values of the instantaneous tail currents derived from a monoexponential fit of the tail current responses. The theoretical Nernst potential of $malate^{2-}$ in 100 mM symmetrical malate conditions is $E_{Nernst}(100\,mM\,MA^{2-}_{cyt}) = 0\,mV$ and in 10 mM cytosolic $malate^{2-}$ concentrations it is $E_{Nernst}(100\,mM\,MA^{2-}_{cyt}) = -28\,mV$. *Error bars* are ±SE

10 mM $malate^{2-}_{cyt}$, the measured reversal potential was +1±1 mV and −29 ± 1 mV, respectively (Fig. 4d). In both cases, these reversal potentials approximate the Nernst potential of $malate^{2-}$ in the investigated conditions ($E_{Nernst}(100\,mM\ malate^{2-}_{cyt} = 0\,mV$ and $E_{Nernst}(100\,mM\ malate^{2-}_{cyt} = -28\,mV$). Therefore, these data show that the current observed in VvALMT9 expressing vacuoles is carried by malate.

VvALMT9 can transport tartrate better than AtALMT9

During the green stage, grape berries accumulate large amounts of MA and TA in the vacuole. Therefore, we were interested in whether VvALMT9 is able to mediate tartrate currents beside malate currents. We conducted a parallel study of TA permeation in AtALMT9 and VvALMT9 (Fig. 5). By exchanging 100 mM $malate^{2-}_{cyt}$ with 100 mM $tartrate^{2-}_{cyt}$, we observed that both VvALMT9 and AtALMT9 expressing vacuoles could mediate tartrate currents. Referring to the malate currents, the tartrate currents had 61 ± 6 % and 48 ± 4 % of the amplitude at −100 mV in VvALMT9 and AtALMT9, respectively (Fig. 5c). Interestingly, the ratio between the currents of tartrate and malate (I_{TA}/I_{MA}) indicates that VvALMT9 is more conductive for tartrate than AtALMT9 (Fig. 5d). Moreover, the current ratio increases with the applied membrane potential (Fig. 5d). This slight voltage

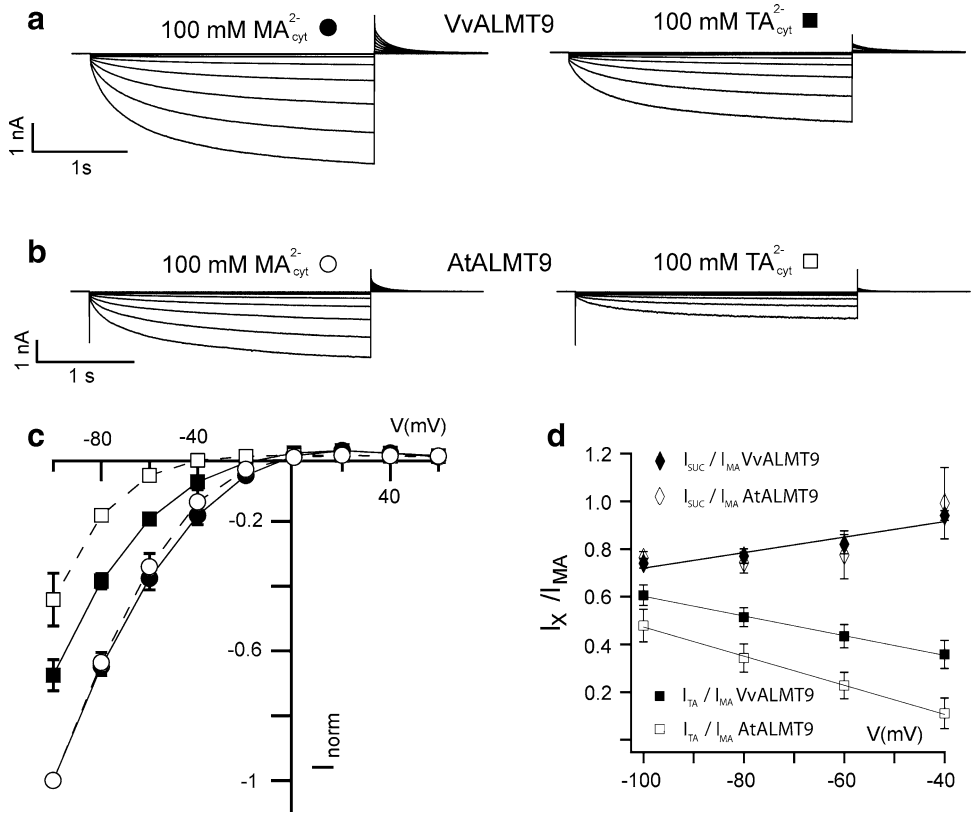

Fig. 5 Comparison between the ion selectivity of VvALMT9 and AtALMT9 for malate and tartrate. **a, b** Representative currents recorded in the presence of 100 mM malate$^{2-}_{cyt}$ (*left traces*) and 100 mM tartrate$^{2-}_{cyt}$ (*right traces*). The cytosolic malate solution was exchanged with a tartrate solution while keeping the same patches from vacuoles overexpressing VvALMT9 (**a**) and AtALMT9 (**b**). Currents were elicited with 3 s voltage pulses ranging from +60 to −120 mV in −20 mV steps followed by a 1.5 s tail pulse at +60 mV The holding potential was +60 mV. **c** Corresponding current amplitude plots derived from excised cytosolic-side-out patches from VvALMT9 overexpressing vacuoles exposed to 100 mM malate (filled circles) and 100 mM tartrate (*filled squares*, $n = 4$), as well as from AtALMT9 overexpressing vacuoles exposed to 100 mM malate (*open circles*; $n = 4$) and 100 mM tartrate (*open squares*; $n = 4$). **d** Ratio between succinate and malate currents mediated by ALMT9 of *V. vinifera* (*filled diamonds*) and *A. thaliana* (*open diamonds*) and ratio between tartrate and malate currents mediated by ALMT9 of *V. vinifera* (*filled squares*) and *A. thaliana* (*open squares*) plotted as a function of the applied membrane potential. *Error bars* denote ±SE

dependency of the I_{TA}/I_{MA} ratio is more pronounced in AtALMT9 than in VvALMT9 (in Fig. 5d the slope of the fitted line is 0.004 mV^{-1} for VvALMT9 and 0.006 mV^{-1} for AtALMT9). Notably, we illustrate in an equally conducted set of experiments that when exchanging from 100 mM malate$^{2-}_{cyt}$ to 100 mM succinate$^{2-}_{cyt}$ that this dicarboxylic acid is likewise transported by VvALMT9 and AtALMT9 (Fig. 5d). The succinate currents were 76 ± 2 and 74 ± 3 % of the currents in malate in VvALMT9 and AtALMT9 at −100 mV, respectively. This indicates that the permeability of succinic acid is identical between the homologous channels of Arabidopsis and *V. vinifera*. In summary, the data show that both VvALMT9 as well as AtALMT9 are slightly less permeable for tartrate than for malate and succinate. Nonetheless, the ratio I_{TA}/I_{MA} provides evidence that VvALMT9 conducts tartrate ions better than AtALMT9. Taken together, these results indicate that both, MA and TA, can be transported in the vacuoles of *V. vinifera* berries through VvALMT9. Hence, VvAtLMT9 is the first malate and tartrate channel identified so far in grape berries.

Discussion

In *V. vinifera*, the accumulation of organic acids in the vacuole is involved in berry development and has a great impact on the final quality of grapes from an agronomical point of view. In this species, the data on the vacuolar transporters involved in the accumulation of MA and TA in berry vacuoles are scarce and no information is available concerning their molecular identity. Based on previous studies in *A. thaliana* (Kovermann et al. 2007; Meyer et al. 2011), we hypothesised that members of the ALMT family

could be involved in the vacuolar accumulation of MA and TA in *V. vinifera* berries. In a preliminary phylogenetic analysis, we found that 13 members of the ALMT family can be identified in the *V. vinifera* genome (Fig. 1). The 13 VvALMTs cluster in three clades that correspond to the clades previously described in Arabidopsis (Kovermann et al. 2007). However, the number of members per clade is different between the two species with clade I being overrepresented and clade III harbouring a single member in *V. vinifera* (Fig. 1). Instead, clade II to which VvALMT9 belongs is represented by a similar number of members in grapevine (Kovermann et al. 2007). We found that when transiently expressed in tobacco leaves, VvALMT9-GFP is localised in the tonoplast as AtALMT9-GFP (Fig. 3a). Further electrophysiological analysis on excised cytosolic-side-out patches of vacuoles obtained from transiently transformed tobacco protoplasts allowed us to demonstrate that VvALMT9 was able to mediate an inward rectifying malate and tartrate current facilitating the accumulation of these dicarboxylic acids in the vacuoles of grape berries (Figs. 4, 5). The comparison between the substrate selectivity properties of VvALMT9 and AtALMT9 reveals that VvALMT9, like AtALMT9, transports malate and succinate better than tartrate (Fig. 5). Nonetheless, VvALMT9 is able to catalyse the transport of TA more efficiently than AtALMT9, which is in contrast to the transport of succinic acid, a metabolic intermediate which is not accumulated substantially in grape berries. This functional difference between the two homologous proteins is intriguing since grape berries are one of the few fruits accumulating significant amounts of TA (Saito and Kasai 1968).

The extremely acidic pH values found in grape vacuoles in the green stage ($\sim$2.5) allow the accumulation of MA and TA via a passive transport system like an anion channel. Indeed, at this pH 99 % of MA and TA are in the fully protonated or monovalent form ($pK_A^{1,MA} = 3.40$, $pK_A^{2,MA} = 5.11$, $pK_A^{1,TA} = 2.98$, $pK_A^{2,TA} = 4.34$; Weast and Astle 1982–1983). The ALMTs are known to mediate only the transport of the divalent form of dicarboxylic acids (Meyer et al. 2011). Hence, in grape berries TA and MA can be taken up from the neutral cytosol across the tonoplast as divalent anions (MA^{2-} and TA^{2-}). Once in the vacuole at pH 2.5, these acids become neutral or monovalent which prevents the conduction by anion channels back to the cytosol. This mechanism, known as ion trapping (Briggs et al. 1987), facilitates loading of grape berry vacuoles with MA and TA (Fig. 6). The unidirectional acid flux might explain the requirement of less anion channels during the green stage compared to the mature grape berry as represented by lower expression levels of VvALMT9 (Fig. 2). The decline in vacuolar acidity observed

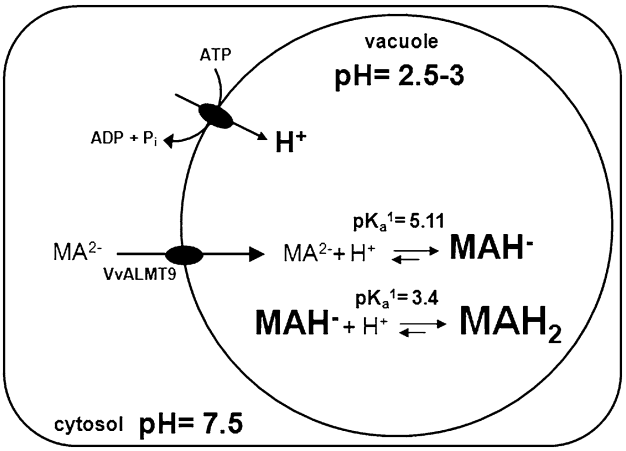

Fig. 6 The ion-trapping mechanism results in vacuolar malate accumulation in grape berries. In the cytosol at pH 7.5, MA is present in its fully deprotonated divalent form malate^{2-} (MA^{2-}). MA^{2-} can be transported by the inward rectifier VvALMT9 into the vacuole. Once in the extremely acidic vacuole of grape berries (pH = 2.5–3), MA^{2-} becomes protonated and accumulates mainly as MAH_2 or in the monovalent form, MAH^-. Both forms of MA are not permeable through ALMTs and thus they are trapped in the vacuolar lumen. The unidirectional flux of malate forms the basic principle of its vacuolar accumulation to high levels. Tartaric acid can be accumulated in the vacuole by the same ion-trapping mechanism since the acidity constants are $pK_A^{1,TA} = 2.98$ and $pK_A^{2,TA} = 4.34$

systematically during grape berry ripening was shown to be accompanied by an increase in tonoplast passive diffusion (Terrier et al. 2001). The up-regulation of global VvALMT expression could consequently be a counteraction for excessive MA and TA decompartementation through anion leakage. Similarly, the rise of mRNA and protein abundance of both vacuolar proton pumps in grape berries during maturation was suggested to partly compensate for passive permeability of the tonoplast (Terrier et al. 2001). A second explanation for the transcriptional up-regulation of VvALMT9 could be an involvement in releasing organic acids from the vacuole during maturation. In late stages of ripening, the vacuolar pH rises to 3.5–4. Under these conditions, a minor proportion of the vacuolar MA would dissociate into the divalent form (MA^{2-}) and be a substrate of VvALMT9. It is therefore possible that the channel catalyses the release of MA^{2-} from the vacuole to the cytosol at this particular phase of development. However, although we cannot exclude this second hypothesis per se, our data demonstrate that anion fluxes mediated by VvALMT9 are directed into the vacuole, thus supporting a role of VvALMT9 in counteracting excessive organic acid decompartementation during maturation.

In conclusion, in the present work we provide evidence that malate and tartrate can be accumulated in the vacuoles of *V. vinifera* berries by VvALMT9. Hence, the present findings represent a step towards understanding

carboxylate metabolism and storage in grapes which are crucial factors impacting wine quality and production.

Acknowledgments We would like to thank Prof. Enrico Martinoia (University of Zurich, Switzerland) for his scientific support and helpful discussions, Dr. Stefan Meyer (University of Zurich, Switzerland) for discussions, Dr. Nelson Saibo (Genomics of Plant Stress Laboratory–ITQB, Universidade Nova de Lisboa, Portugal) for kindly providing the cloning vectors and Duarte Figueiredo (Genomics of Plant Stress Laboratory–ITQB, Universidade Nova de Lisboa), Tânia Serra (Genomics of Plant Stress Laboratory–ITQB, Universidade Nova de Lisboa) and André Cordeiro (Genomics of Plant Stress Laboratory–ITQB, Universidade Nova de Lisboa) for technical support with the preliminary *Nicotiana* agroinfiltration experiments. AR and RF acknowledge FCT for the financial support through fellow FRH/BPD/34986/2007 and SFRH/BPD/74210/2010, respectively. AD was supported by a long-term EMBO fellowship (ALTF 87-2009), JZ by the Chinese Scholarship Council and UB by the Swiss National Foundation (31003A_141090/1).

References

Briggs GG, Rigitano RLO, Bromilow RH (1987) Physico-chemical factors affecting uptake by roots and translocation to shoots of weak acids in barley. Pestic Sci 19:101–112

Conde C, Silva P, Fontes N, Dias ACP, Tavares RM, Sousa MJ, Agasse A, Delrot S, Geros H (2007) Biochemical changes throughout grape berry development and fruit and wine quality. Food 1:1–22

Coombe BG (1976) The development of fleshy fruits. Annu Rev Plant Physiol 27:207–228

Coombe BG (1992) Research on development and ripening on the grape berry. Am J Enol Vitic 43:101–110

Emmerlich V, Linka N, Reinhold T, Hurth MA, Traub M, Martinoia E, Neuhaus HE (2003) The plant homolog to the human sodium/dicarboxylic cotransporter is the vacuolar malate carrier. Proc Natl Acad Sci USA 100:11122–11126

Fernie AR, Martinoia E (2009) Malate: Jack of all trades or master of a few? Phytochemistry 70:828–832

Hoekenga OAL, Maron G, Piñeros MA, Cançado GM, Shaff J, Kobayashi Y, Ryan PR, Dong B, Delhaize E, Sasaki T, Matsumoto H, Yamamoto Y, Koyama H, Kochian LV (2006) *AtALMT1*, which encodes a malate transporter, is identified as one of several genes critical for aluminum tolerance in *Arabidopsis*. Proc Natl Acad Sci USA 103:9738–9743

Holsters M, Silva B, Van Vliet F, Genetello C, De Block M, Dhaese P, Depicker A, Inzé D, Engler G, Villarroel R (1980) The functional organization of the nopaline *A. tumefaciens* plasmid pTiC58. Plasmid 3:212–230

Kanellis AK, Roubelakis-Angelakis KA (1993) Grapes. In: Seymour GI, Taylor J, Tucker GA (eds) Biochemistry of fruit ripening. Chapman & Hall, London, pp 189–234

Kovermann P, Meyer S, Hörtensteiner S, Picco C, Scholz-Starke J, Ravera S, Lee Y, Martinoia E (2007) The Arabidopsis vacuolar malate channel is a member of the ALMT family. Plant J 52:1169–1180

Melino VJ, Soole KL, Ford CM (2009) Ascorbate metabolism and the developmental demand for tartaric and oxalic acids in ripening grape berries. BMC Plant Biol 9:145

Meyer S, Mumm P, Imes D, Endler A, Weder B, Al-Rasheid KA, Geiger D, Marten I, Martinoia E, Hedrich R (2010) *At*ALMT12 represents an R-type anion channel required for stomatal movement in Arabidopsis guard cells. Plant J 63:1054–1062

Meyer S, Scholz-Starke J, De Angeli A, Kovermann P, Burla B, Gambale F, Martinoia E (2011) Malate transport by the vacuolar AtALMT6 channel in guard cells is subject to multiple regulation. Plant J 67:247–257

Pfaffl MW (2001) A new mathematical model for relative quantification in real-time RT-PCR. Nucleic Acids Res 29(9):e45

Reid KE, Olsson N, Schlosser J, Peng F, Lund ST (2006) An optimized grapevine RNA isolation procedure and statistical determination of reference genes for real-time RT-PCR during berry development. BMC Plant Biol 6:27

Saito K, Kasai Z (1968) Accumulation of tartaric acid in the ripening process of grapes. Plant Cell Physiol 9:529–537

Saito K, Kasai Z (1969) Tartaric acid synthesis from l-ascorbic acid-1-^{14}C in grape berries. Phytochemistry 8:2177–2182

Sweetman C, Deluc G, Cramer GR, Ford CM, Soole KL (2009) Regulation of malate metabolism in grape berry and other developing fruits. Phytochemistry 70:1329–1344

Taureilles-Saurel C, Romieu CG, Robin JP, Flanzy C (1995a) Grape (*Vitis vinifera* L.) malate dehydrogenase. I. Intracellular compartmentationof the isoforms. Am J Enol Vitic 46:22–28

Taureilles-Saurel C, Romieu CG, Robin JP, Flanzy C (1995b) Grape (*Vitis vinifera* L.) malate dehydrogenase. II. Characterization of the major mitochondrial and cytosolic isoforms and their role in ripening. Am J Enol Vitic 46:29–36

Terrier N, Sauvage FX, Ageorges A, Romieu C (2001) Changes in acidity and in proton transport at the tonoplast of grape berries during development. Planta 213:20–28

Thompson JD, Higgins DG, Gibson TJ (1994) CLUSTAL W: improving the sensitivity of progressive multiple sequence alignment through sequence weighting, position-specific gap penalties and weight matrix choice. Nucleic Acids Res 22:4673–4680

Weast RC, Astle MJ (1982–1983) CRC Handbook of chemistry and physics. CRC Press. Boca Raton